Heliyon 6 (2020) e03887

Contents lists available at ScienceDirect

Heliyon

journal homepage: www.cell.com/heliyon

Research article

Turpentine valorization by its oxyfunctionalization to nopol through heterogeneous catalysis

Iván Aguas, Edwin Alarcón *, Aída Luz Villa

Universidad de Antioquia, Chemical Engineering Department, Environmental Catalysis Research Group, Calle 70 No. 52-21, Medellín, Colombia

ARTICLE INFO

Keywords:
Chemical engineering
Organic chemistry
β-pinene
Turpentine
Nopol
Prins reaction
Sn-MCM-41

ABSTRACT

Turpentine is a mixture of monoterpene hydrocarbons obtained as a by-product in the paper industry. In this contribution we present its transformation process towards an alcohol named nopol, that is an important household product and fragrance raw material. Reaction conditions were established for the oxyfuntionalization of crude turpentine oil over Sn-MCM-41 catalyst for the selective conversion of β-pinene to nopol. Synthesized materials were characterized by XRD, N_2 adsorption, FT-IR, TEM and chemical absorption. The reaction was tested in 2 mL glass reactor with a sample of commercial turpentine with α-pinene (55.5% w/w) and β-pinene (39.5% w/w) as main components and scaled up into a 100 mL Parr reactor, getting 92% conversion of β-pinene and a nopol selectivity of 93%. The reusability tests showed that the catalyst can be reused 4 times without loss of activity. The results showed that 86% less solvent and 37.5% less paraformaldehyde can be used with turpentine, compared to the conditions used with β-pinene for getting similar catalysts activity.

1. Introduction

Crude sulfate turpentine is one of the kraft pulping process byproducts of pine wood. It is a cheap material with applications in the manufacture of solvents and cleaning materials [1]. Many perfume chemicals are produced from α-pinene and β-pinene, the main constituents of turpentine [1]. Nopol, 2-(7,7-dimethyl-4-bicyclo [3.1.1] hept-3-enyl) ethanol, is an added-value chemical synthesized through Prins reaction between paraformaldehyde and β -pinene [2]. This alcohol is used in household product formulations, agrochemicals, detergents and soaps [3]. Some of the widely used processes for the production of nopol require temperatures around 200 °C or the use of homogeneous catalysts such as $ZnCl_2$ [4,5].

The above methods present some drawbacks, due to their low selectivity to nopol, high energy demand, the use of toxic and corrosive chemicals, the elimination of complex chemical residues or the difficulty in separating the catalyst from the reaction mixture [6, 7]. For this reason, different heterogeneous catalytic systems have been studied for the production of nopol, such as Sn-SBA-15, sulfated zirconia and Sn-MCM-41 [7, 8, 9, 10, 11]. Using a more efficient catalyst such as Sn-MCM-41 for the transformation of β-pinene, is possible to reduce the temperature of the process below 100 °C with the additional advantage of ease separation and reuse of the catalyst. Over Sn-MCM-41, yields between 90 and 100% have been reported [12, 13, 14, 15], values that exceed the optimum yield reported (71%) with the homogeneous catalyst $ZnCl_2$ [4]. The mesoporous properties (large surface area with pores diameters between 1.5 to 10 nm [16] and a thin pore-walls of 1–1.5 nm [17]) of the MCM-41 allow the diffusion of the β-pinene molecule into the large pore sizes that facilitate they reach the active tin species. Additionally, tin generate Lewis-type acidity that is required to carry out the condensation of Prins between β -pinene and formaldehyde [18].

In this contribution, the use of Sn-MCM-41 catalyst in the oxyfunctionalization of commercial turpentine (50% α-pinene, 40% β-pinene, 3% limonene, 7% other monoterpenes) as source of β-pinene is studied using different amounts of ethyl acetate as a solvent, for avoiding formaldehyde polymerization in the vapor phase [19]. An efficient and environmentally friendly process is looked for adding value to the kraft pulping process byproducts of pine wood and contribute to green chemistry standards.

2. Materials and methods

2.1. Materials

The reagents used in this work were β-pinene (purity 99% w/w), myristyltrimethylammonium bromide (purity 99% w/w), tetraethyl

* Corresponding author.
E-mail address: edwin.alarcon@udea.edu.co (E. Alarcón).

https://doi.org/10.1016/j.heliyon.2020.e03887
Received 22 December 2018; Received in revised form 7 April 2020; Accepted 28 April 2020
2405-8440/© 2020 Published by Elsevier Ltd. This is an open access article under the CC BY-NC-ND license (http://creativecommons.org/licenses/by-nc-nd/4.0/).

orthosilicate (TEOS, 98% w/w), paraformaldehyde (purity 95% w/w) supplied by Sigma Aldrich; $SnCl_2{\cdot}2H_2O$ supplied by Alfa Aesar; aqueous ammonia (28–30% w/w) supplied by EM Science; toluene (99.9% w/w) and ethyl acetate (purity 99.5% w/w) were purchased to J. T. Barker. Commercial turpentine oil was obtained from local market.

2.2. Catalyst synthesis

MCM-41 was prepared using the method reported by Grün et al [20]. Briefly, myristyl trimethylammonium bromide was dissolved in distilled water under vigorous stirring. Then, the pH was adjusted by adding aqueous ammonia and TEOS was added dropwise at 10 mL min^{-1}, using a peristaltic pump. This suspension was stirred at room temperature for 1 h. The precipitate was filtered and dried overnight at 100 °C. The solid obtained was calcined at 550 °C for 5 h (1 °C min^{-1}).

Sn was grafted onto the mesoporous materials via incipient wetness impregnation [7, 10]. A solution of $SnCl_2{\cdot}2H_2O$ in ethyl acetate was prepared and added to the solid dropwise and under a manual homogenization process. The solid obtained was dried for 24 h at room temperature and calcined at 550 °C for 5 h (1 °C min^{-1}).

2.3. Catalyst characterization

The phase structures of the catalyst were identified by small angle XRD analysis in a Bruker AXS diffractometer provided with a copper lamp, monochromatic CuKα radiation source (λ = 1.5406 Å). The porous properties of the samples were determined by N_2 sorption isotherms at 77 K using a Micrometics model ASAP 2020 PLUS. Surface areas were calculated using the Brunauer-Emmett-Teller (BET) method and Barrett-Joyner- Halenda (BJH) pore size distribution from the desorption branch. The FTIR measurements were carried out by mixing the powder sample with KBr, in a Frontier FT-IR spectrometer (PerkinElmer), model Spectrum 65, with a resolution of 4 cm^{-1}. Transmission electron microscopy (TEM) images were collected on a Tecnai F20 Super Twin Transmission Electronic Microscope TMP by FEI. The Sn content was quantified by chemical absorption in a Thermo Elemental spectrometer SOLAAR S4 Spectrometer.

2.4. Catalytic reactions

First, reactions were performed at 90 °C with pure β-pinene in 2 mL vials covered with inert silicon septa equipped with magnetic stirrer at 2000 rpm, immersed in an oil bath whose temperature was controlled with an IKA brand FUZZY temperature controller [13, 14]. A stirring speed of 2000 rpm was used for avoiding external mass transfer limitations, as it was reported for nopol synthesis by Prins condensation of pure β-pinene and paraformaldehyde over Sn-MCM-4 [21]. The average particle size of the catalyst used was between 38 and 41.5 μm for avoiding internal mass transfer limitations. Later, a commercial turpentine sample was characterized and used instead of high purity β-pinene to evaluate the effect of different reaction parameters such as the amount and type of solvent, the amount of catalyst and the reaction time; appropriate reaction conditions were obtained (12 mg Sn-MCM-41, 0.8 mmol of β-pinene from commercial turpentine, 1 mmol of paraformaldehyde (HCHOx), 0.25 mL of ethyl acetate, 90 °C). Larger scale reaction in a 100 mL Parr reactor was evaluated.

Reaction products were analyzed using a gas chromatograph model 7890 N Agilent, coupled with a mass Triple-Axis detector (5975C, Agilent). The GC was equipped with a DB-1 capillary column (30 m × 320 μm x 0.25 μm) and the carrier gas was helium. The chromatograph oven temperature was kept at 100 °C for 1 min, and then it was increased to 220 °C at a rate of 10 °C min^{-1}, where it remained stable for 1 min; the split ratio was 1/25. The GC-MS operates simultaneously with a MS-source temperature of 230 °C and MS-quadrupole temperature of 150 °C. The system was operated in electron impact mode and the MS spectra were analyzed using the NIST library.

Pure nopol was identified by comparison with standard sample and by GC-MS. The analysis of the reaction samples was carried out by the external standard method: three calibration curves corresponding to α-pinene, β-pinene and nopol were prepared; the samples of known concentration were prepared in volumetric balloons of 5 mL, which was later analyzed by gas chromatography. Molar concentrations were plotted against the average area obtained by chromatographic analysis. The quantification was carried out by comparing the signals of the sample with those corresponding to the standard solutions. Catalyst recycling study was carried out to check the heterogeneity of the catalyst.

The conversion, selectivity and yield were calculated using Eqs. (1), (2), and (3), respectively.

$$\%\,\beta - Pinene\ conversion = \frac{\left(C_{\beta-pinene}\right)_{initial} - \left(C_{\beta-pinene}\right)_{final}}{\left(C_{\beta-pinene}\right)_{initial}} * 100 \quad (1)$$

$$\%\,Nopol\ selectivity = \frac{C_{nopol}}{\left(C_{\beta-pinene}\right)_{initial} - \left(C_{\beta-pinene}\right)_{final}} * 100 \quad (2)$$

$$\%\,Nopol\ yield = \frac{\%\,\beta - pinene\ conversion * \%nopol\ selectivity}{100} \quad (3)$$

where C is the concentration.

3. Results and discussion

3.1. Catalyst characterization

Typical powder X-ray diffraction pattern of MCM-41 and Sn-MCM-41 samples are shown in Figure 1. The literature reports that materials of mesoporous channels with hexagonal distribution are characterized by a pronounced reflection at 2θ = 2°, and two small reflections at higher angles [20, 22]. The synthesized materials have the characteristic peak at 2θ = 2.6°, which corresponds to the reflection of the d_{100} ~ 33 Å plane [23]. The diffractogram of MCM-41 (Figure 1a) shows the four characteristic signals of this materials as (100), (110), (200) and (210) reflections [16], as well as the tin catalyst (Figure 1b) which has the same peaks but with a decrease in its intensity. This phenomenon, as well as the displacement at greater angles, has been observed previously [13, 24], and has been attributed to the slight distortion of the hexagonal array of channels of the MCM-41 incorporating other species such as Sn and Zn, and the decrease of the cell parameters when removing the structuring agent.

Figure 2 shows N_2 adsorption-desorption isotherms of the MCM-41 and Sn-MCM-41 materials. The isotherms of both samples were type IV according to the IUPAC classification, a typical type for small pore diameter mesoporous materials without a visible an H1 hysteresis loop [10, 25]. Table 1 shows the BET surface area, the pore volume and the pore diameter and the Sn content of the synthesized materials. When comparing the BET area obtained for MCM-41 and Sn-MCM-41, it is possible to concluded that they are within the range reported in previous studies for this kind of materials, 929–1154 $m^2\ g^{-1}$ [24]. In this case the physical properties are not drastically affected because tin incorporation.

The atomic absorption analysis (Table 1) showed that the Sn content (0.25% w/w or 21 μmol Sn g^{-1} of catalyst) of the synthesized material, is very similar to the value reported in previous studies for Sn-MCM-41 (24 μmol Sn/g of catalyst) [15].

The IR spectra for synthesized MCM-41, MCM-41 after calcination and Sn-MCM-41 are shown in Figure 3. The peaks around 1500 cm^{-1} assigned to aliphatic C–H bending vibrations and 2930 cm^{-1} assigned to aliphatic C–H stretching vibrations of the surfactant disappear during the calcination process [26], which indicates that the surfactant was effectively removed from the MCM-41. The band around 3432 cm^{-1} in the three materials could be related to O–H bond stretching vibrations [27]. The bands around 1629 cm^{-1} are caused by the vibrations of water

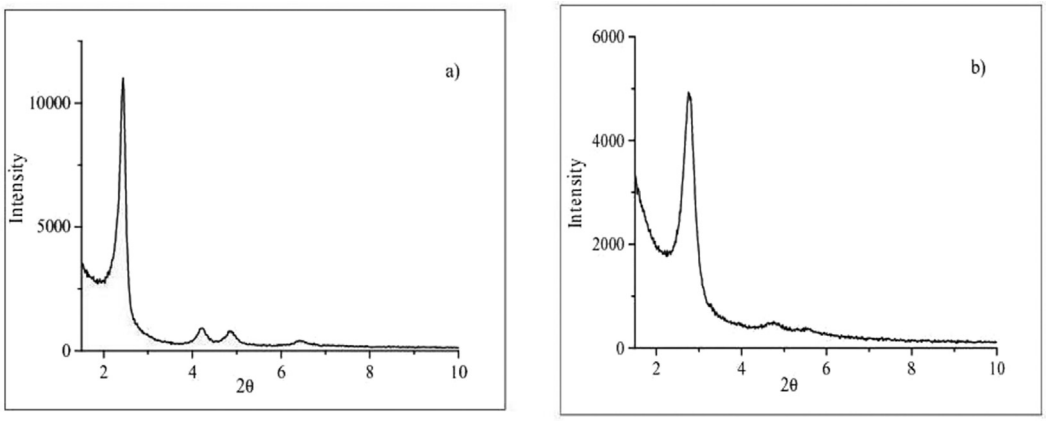

Figure 1. XRD patterns of synthesized materials (a) MCM-41 (b) Sn-MCM-41.

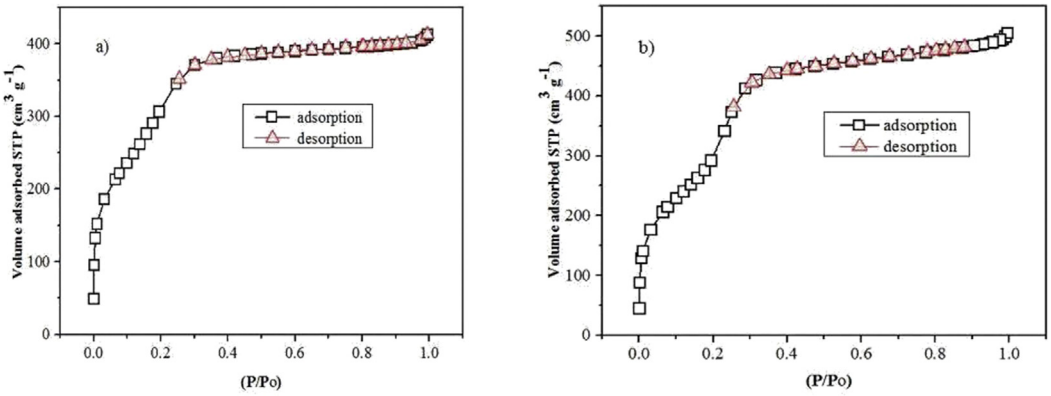

Figure 2. N_2 adsorption-desorption isotherms of (a) MCM-41 and (b) Sn-MCM-41.

molecules, while the bands close to 1080 cm^{-1} could represent the bending and symmetric stretching vibrations of the Si–O–Si linkages [27, 28]. This assignment of characteristic bands of the MCM-41 confirms the results found by XRD sown in Figure 1. The characteristic bands of the MCM-41 (1080 cm^{-1}) [27], indicates that the process of silica formation was successfully carried out; while the appearance of aliphatic C–H bending and stretching vibrations (1629 cm^{-1}, 2930 cm^{-1}) [28], may be owing to no hydrolyzed TEOS. When metal is introduced into the support structure, distinctive bands appear at 968 cm^{-1}, which corresponds to stretching vibration of heteroatom attached to Si–O–Sn [29, 30]. In this case, there are no distinctive bands that suggest the incorporation of tin in the structure.

Figure 4 shows the TEM images for MCM-41 and Sn-MCM-4. As can be observe there is a well-ordered hexagonal arrangement structure in both materials [24]. No agglomerates are observed, suggesting an adequate method of synthesis for MCM-41 and a uniform distribution of deposited tin.

Table 1. Physical properties of MCM-41 and Sn-MCM-41 materials.

Property	MCM-41	Sn MCM-41
µmol Sn/g support[a]		43.05
%w/w Sn Deposited[b]		0.25
BET Surface Area (m^2/g)	1041	1043
Pore volume (cm^3 g^{-1})	0.64	0.77
Pore diameter D_{BJH} (nm)	3.47	3.29

[a] Amount of tin used in the impregnation procedure.
[b] Tin charge determined by atomic adsorption.

3.2. Catalytic reactions

First, the activity of the catalyst was evaluated under the standard reaction conditions between β-pinene and paraformaldehyde in the presence of ethyl acetate (12 mg of Sn-MCM-41, β-pinene in ethyl acetate solution 0.46 M (1 mL), (HCHO)x:β-pinene molar ratio of 2:1, 90 °C, 0.5 h) where a conversion of 40% and a selectivity to nopol of 93% were reported [15]. The catalytic reactions using Sn-MCM-41 synthesized for this work showed a conversion of 25.2%, selectivity of 89.8% and a yield of 22.6%. These results show a conversion 10 units below the reported one, which may be associated to the actual amount of Sn deposited. The reference reports a tin charge of 24 µmol Sn g^{-1} catalyst, while the material used in this work has 21 µmol Sn g^{-1} of catalyst, which translates to 12.5% w/w less than the reference. Studies show that the metal content and the pore size can affect the catalytic performance of Sn-MCM-41 materials [10].

One advantage of this process is the use of the heterogeneous catalyst Sn-MCM-41. Table 2 shows the TOF values for three different catalysts in the production of nopol under the same reaction conditions. Sn-MCM-41 and $ZnCl_2$ have a comparable catalytic activity. However, the heterogeneous catalyst is easier to separate from the reaction mixture and can be reused without loss of activity. Although, higher conversion is obtained using $SnCl_2$ as catalyst, its lower selectivity suggests a more complex process for nopol separation.

Two samples of turpentine from different suppliers were characterized by gas chromatography. The samples were named sample TE-1 and TP-1 and characterized using peak area normalization method (Table 3).

Figure 5 shows the chromatograms for both turpentine samples. The peaks assigned to 5.2 and 5.5 min correspond to α-pinene and β-pinene,

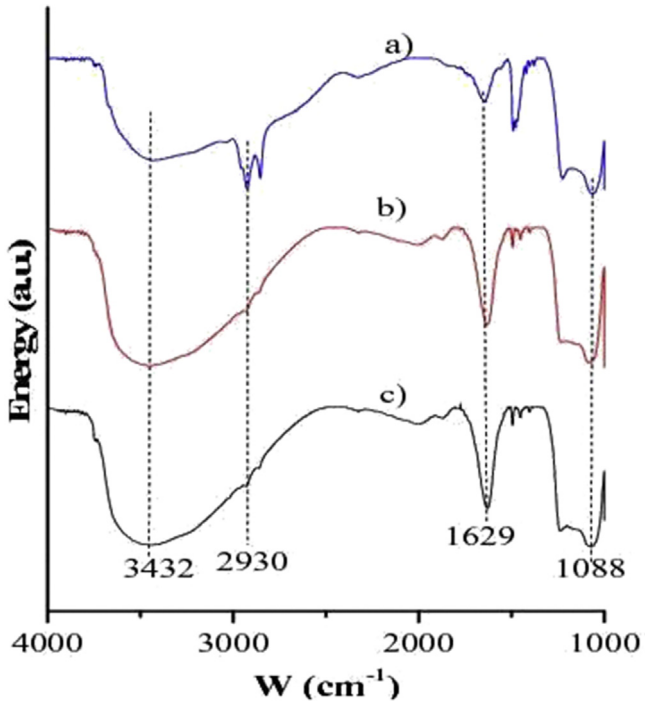

Figure 3. FTIR spectra of (a) MCM-41without calcination, (b) calcinated MCM-41 and (c) Sn-MCM-41 materials.

respectively. From the figure it can be concluded that the sample TP-1 has a higher content of α-pinene, while the sample TE-1 has a higher content of β-pinene. The results of the analysis by the external standard method showed that sample TE-1 had 55.45% w/w of α-pinene, 39.5% w/w of β-pinene and others, while TP-1 has 78.78% and 9.99% w/w of α and β-pinene, respectively. The results found by the external standard method are very similar to those found by the normalization of areas (Table 3). Therefore, it was decided to use the sample with the highest β-pinene content for the reaction tests.

Figure 6 shows the effect of the amount of two different solvents (*n*-heptane and ethyl acetate) on conversion of β-pinene that contains the turpentine sample and selectivity and yield of nopol [7]. Figure 6a shows that as the amount of *n*-heptane increases, the selectivity of the reaction

Table 2. Comparison of TOF between homogeneous and heterogeneous catalysts.

Catalyst	% Conversion	% Selectivity	TOF[a]
Sn-MCM-41	40	98	0.0025
$SnCl_2$	98	85	0.0048
$ZnCl_2$	91	92	0.0028

Reaction conditions: Catalyst (12 mg), β-pinene (0.46 mmol), HCHOx (1 mmol), 30 min, 1 mL ethyl acetate, 90 °C [a] mol of substrate converted/(mol Sn s).

toward nopol increases; however, the conversion and yield decrease. When ethyl acetate was used as a solvent for the oxyfuntionalization of turpentine (Figure 6b), better results were obtained. The polarity of the solvent may affect also the reaction rate. A polar solvent can positively affect the reaction rate by coordinating and stabilizing the intermediate carbocation [7]. n-Heptane is a non-polar solvent with a relative polarity of 0.012 while ethyl acetate is an aprotic apolar solvent with a relative polarity of 0.228, the low polarity of the n-heptane could decrease the coordination of the intermediate species and causes a decrease in the reaction rate [31]. The kinetics and the effect of solvent was previously described [7] and it was found that solubility of formaldehyde was higher in ethyl acetate than in toluene that has a lower polarity. When there is not ethyl acetate and α-pinene (that is the main component of turpentine oil) plays the solvent role, conversion is low. The maximum of conversion is obtained in Figure 6b when ethyl acetate is added because formaldehyde solubility enhances, but then conversion decreases because the rate law giving in Eq. (4) [7] indicates that an increase on the concentration of solvent will reduce the catalytic activity.

$$r = \frac{k_{rs} K_A K_B C_A C_B}{\left(1 + K_A C_A + K_B C_B + K_C C_C + K_{sol} C_{sol}\right)^2} \quad (4)$$

The best results were found using 0.25 mL of ethyl acetate, a conversion of 40% and a selectivity of approximately 75% were obtained.

Figure 7a shows that although the reaction can be carried out in the absence of solvent, higher yields are achieved in the presence of ethyl acetate, and without paraformaldehyde deposits in the cold reactor zones, which is due to the fact that polymerization of formaldehyde in vapor phase is favored thermodynamically at temperatures below 80 °C [19]. It was observed that an increase in the amount of catalyst enhances the conversion (Figure 7b), however the selectivity seems to decrease when the catalyst concentration is doubled. Possibly it is an effect caused

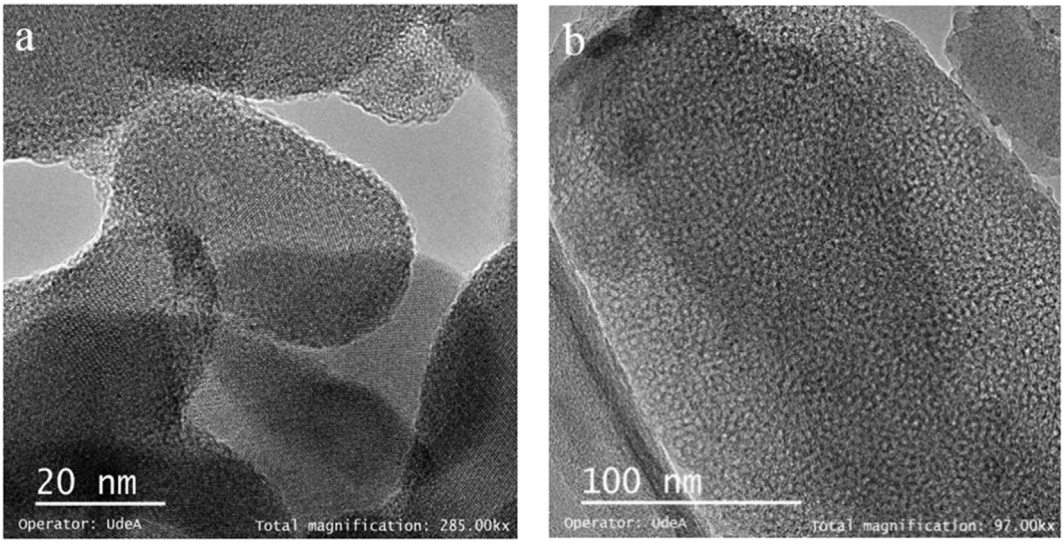

Figure 4. TEM images of (a) MCM-41 and (b) Sn-MCM-41.

Table 3. Characterization of turpentine samples using peak area normalization method.

Sample TE-1		Sample TP-1	
Name	% w/w	Name	% w/w
α-Pinene	50.0	α-Pinene	67.1
Camphene	1.3	Camphene	1.3
β-Pinene	40.5	β-Pinene	13.7
Sabinene	0.4	(+)-3-Carene	2.6
p-Cimene	0.9	Limonene	2.7
γ-Terpinene	4.8	α-Phellandrene	1.8
Fenchone	0.2	*trans*-Pinocarveol	0.3
α-Pinene epoxide	0.1	(+)-4-Carene	1.7
Fenchol	0.4	α-Longipinene	0.7
Terpinen-4-ol	0.1	α-Santalene	0.4
α-Terpineol	0.4	Sativene	0.3
Borneol	0.2	Longifolene	6.1
Unidentified	0.9	Unidentified	1.3

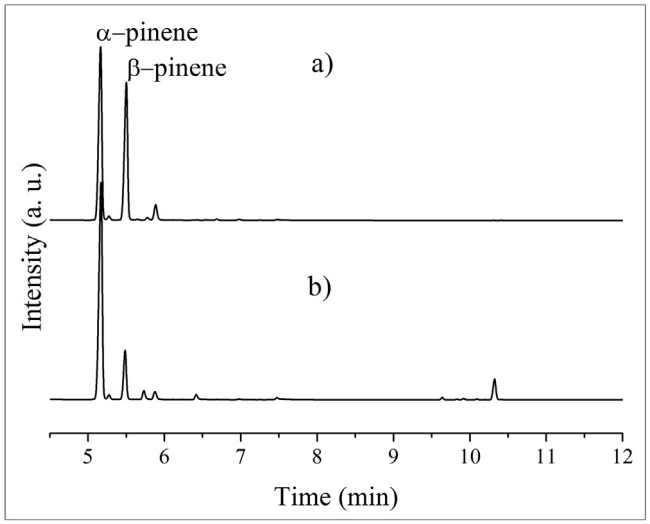

Figure 5. Chromatographic analysis of two turpentine samples. (a) TE-1 and (b) TP-1.

by the competitive absorption between the different components of turpentine or simply as time progresses the catalyst becomes less efficient and the selectivity begins to decrease due to secondary reactions catalyzed by Lewis acid sites. Some changes were found in the areas of the isomers such as limonene, a behavior that has been previously reported [32]. The results show that 86% less solvent and 37.5% less paraformaldehyde can be used with turpentine, compared to the conditions used with pure β-pinene.

Finally, the reaction was carried out in a 100 mL Parr 4590 reactor, for 24 h, in order to determine if it is possible to scale the oxyfunctionalization process without affecting the conversion and selectivity. Then, ethyl acetate was separated from the sample by means of a rotoevaporation process at 85 °C and 500 mbar Figure 8 shows the turpentine spectra before and after the oxyfunctionalization process. A conversion of 92% for β-pinene and 93% of selectivity to nopol were obtained. The final composition by weight of the sample of oxygenated turpentine was 42.7% nopol, 2.37% β-pinene, 51.73% α-pinene and others was obtained.

3.3. Reusability tests

The performance and viability of a heterogeneous catalyst is also measured by its capacity for been reused. The reuse of Sn-MCM-41 was evaluated in 2 mL vials under the same reaction conditions used with turpentine as substrate. After each use, the material was washed twice with 2-propanol under magnetic stirring for 30 min and then washed with ethyl acetate for an additional 30 min; and finally dried at 100 °C for 12 h. Figure 9 shows that the catalyst activity is maintained after reusing the catalyst four times; which demonstrates the good performance of the catalyst and suggests a remarkable chemical stability of the metal on the surface of the support.

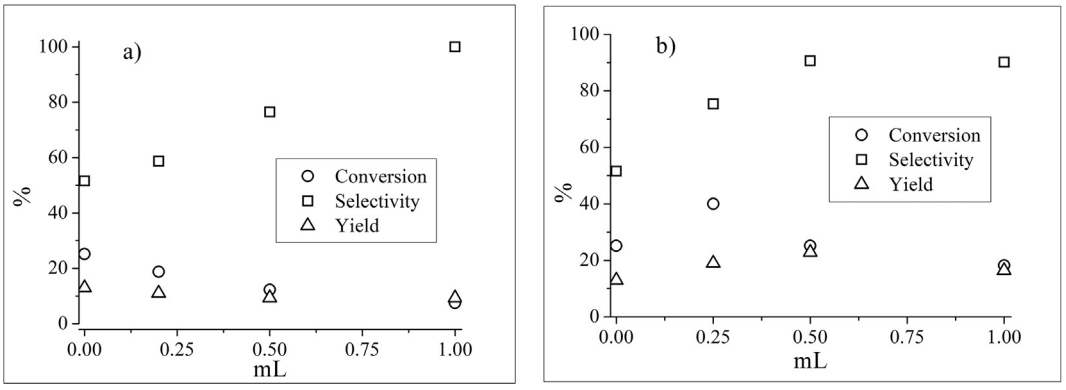

Figure 6. Effect of the amount of (a) *n*-heptane and (b) ethyl acetate on β-pinene conversion, nopol selectivity and nopol yield. Reaction conditions: Sn-MCM-41 (12 mg), β-pinene (0.8 mmol), HCHOx (1 mmol), turpentine with 39.5% w/w of β-pinene, 1 h, 90 °C.

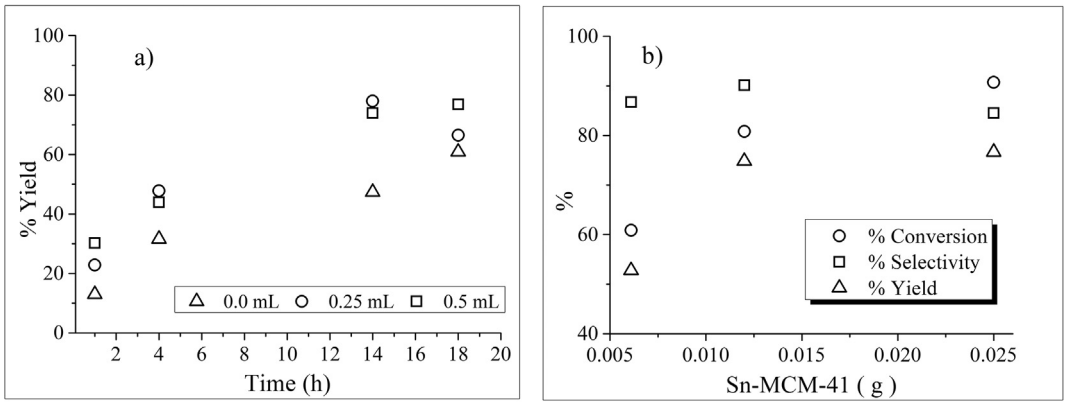

Figure 7. Effect of (a) amount of solvent and (b) amount of catalyst on the oxyfunctionalization of turpentine. Reaction conditions: catalyst (12 mg), turpentine with 39.5% w/w of β-pinene (0.8 mmol), HCHOx (1 mmol), 90 °C, ethyl acetate as solvent.

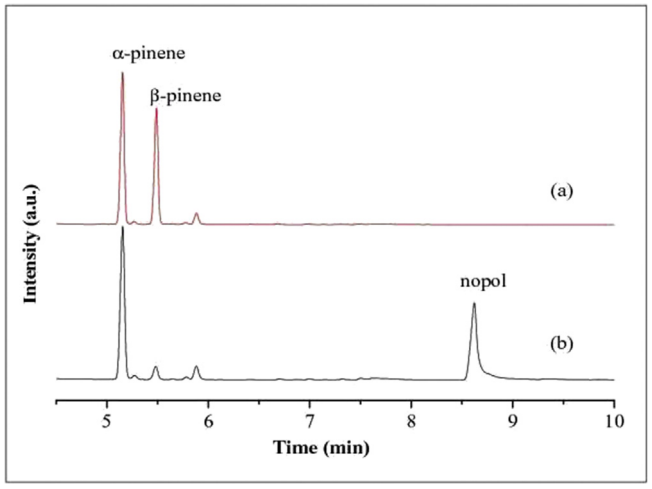

Figure 8. Chromatographic analysis of turpentine before (a) and after oxyfunctionalization by reaction of Prins with paraformaldehyde (b). Reaction conditions scaled up to 50 times: Catalyst (12 mg), β-pinene (0.8 mmol), HCHOx (1 mmol), 90 °C, 0.25 mL of ethyl acetate.

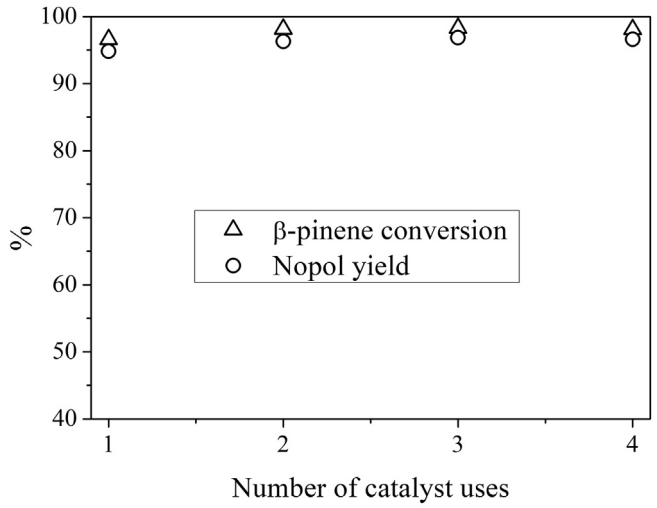

Figure 9. Reusability tests in turpentine. Reaction conditions: 12 mg Sn-MCM-41, β-pinene in turpentine (0.8 mmol), HCHOx (1 mmol), 18 h, 90 °C, 0.25 mL of ethyl acetate.

4. Conclusions

The selective condensation of β-pinene present in turpentine sample over the catalyst Sn- MCM-41 was successfully carried out. Turpentine oil can be oxyfunctionalized to the nopol molecule with high yield (81%) and selectivity (92) after 24 h. Using 75% less solvent and 37.5% less amount of paraformaldehyde, compared to the conditions normally used with pure β-pinene. The oxyfunctionalization could be scaled without requiring drastic modifications, using a Parr 4590 reactor of 100 mL for 24 h to obtain a conversion of 92% and 93% selectivity to nopol, with a mass composition of the main components of 42.7% nopol, 2.37 % of β-pinene and 51.73% of α-pinene. This process gives added value to oxyturpentine and reduces the risk of contamination generated by homogeneous catalysts during the traditional nopol synthesis processes. The results show that 86% less solvent and 37.5% less paraformaldehyde can be used with turpentine, compared to the conditions used with β-pinene for getting the same activity. These favorable conditions allows to process the essential oil under milder and economical conditions, using the catalyst 4 more times.

Declarations

Author contribution statement

Ivan Aguas: Conceived and designed the experiments; Performed the experiments; Analyzed and interpreted the data; Wrote the paper.

Edwin Alarcón: Conceived and designed the experiments; Analyzed and interpreted the data; Wrote the paper.

Aída Luz Villa: Analyzed and interpreted the data; Contributed reagents, materials, analysis tools or data; Wrote the paper.

Funding statement

Edwin Alarcon was supported by Minciencias, Ministerio de Ciencia, Tecnología e Innovación (Project 111574558199 Contract 001-2017).

Ivan Aguas was supported by Minciencias, Ministerio de Ciencia, Tecnología e Innovación ("Convocatoria Nacional Jóvenes Investigadores e Innovadores" call 645).

Competing interest statement

The authors declare no conflict of interest.

Additional information

No additional information is available for this paper.

References

[1] H. Pakdel, S. Sarron, C. Roy, α-Terpineol from hydration of crude sulfate turpentine oil, J. Agric. Food Chem. 49 (2001) 4337–4341.

[2] I.M. Pastor, M. Yus, The prins reaction: advances and applications, Curr. Org. Chem. 11 (2007) 925–957.

[3] J. Wang, S. Jaenicke, G. Khuan, W. Hua, Y. Yue, Z. Gao, Acidity and porosity modulation of MWW type zeolites for Nopol production by Prins condensation, Catal. Commun. 12 (2011) 1131–1135.

[4] J. Bain, The reaction of β-pinene with formaldehyde, J. Am. Chem. Soc. 68 (1946) 638–641.

[5] L.X.Y. Feng-ping, L.- Wei-guang, Z. Yong-hong, Study on synthesis of nopol by closed-vessel and catalyst, J. Guangxi Univ. Nat. Sci. Ed. 26 (2001) 108–111.

[6] J.R. Patil MV, M.K. Yadav, Prins condensation for synthesis of nopol from β-pinene and paraformaldehyde on novel Fe–Zn double metal cyanide solid acid catalyst, J. Mol. Catal. Chem. 273 (2007) 39–47.

[7] D. Casas-Orozco, E. Alarcón, A.L. Villa, Kinetic study of the nopol synthesis by the Prins reaction over tin impregnated MCM-41 catalyst with ethyl acetate as solvent, Fuel 149 (2015) 130–137.

[8] V. Ramaswamy, P. Shah, K. Lazar, A.V. Ramaswamy, Synthesis, characterization and catalytic activity of Sn-SBA-15 mesoporous molecular sieves, Catal. Surv. Asia 12 (2008) 283–309.

[9] S. Jadhav, K.M. Jinka, H.C. Bajaj, Nanosized sulfated zinc ferrite as catalyst for the synthesis of nopol and other fine chemicals, Catal. Today (2012) 98–105.

[10] D. Casas-Orozco, E. Alarcón, C. Carrero, J.M. Venegas, W. McDermott, E. Klosterman, I. Hermans, A.L. Villa, Influence of tin loading and pore size of Sn/MCM-41 catalysts on the synthesis of nopol, Ind. Eng. Chem. Res. 56 (2017) 6590–6598.

[11] W. Xueyan, T. Wang, W. Hua, Y. Yinghong, G. Zi, Synthesis of zirconia porous phosphate heterostructures (Zr-PPH) for Prins condensation, Catal. Commun. 43 (2014) 97–101.

[12] E.A. Alarcón, A.L. Villa, Síntesis de nopol a partir de trementina: revisión del estado del arte, Ing. Cienc. 8 (2012) 281–305.

[13] A.L. Villa, E. Alarcón, C. Montes de Correa, Synthesis of nopol over MCM-41 catalysts, Chem. Commun. (2002) 2654–2655.

[14] E. Alarcón, Síntesis de Nopol a partir de Aceite de Trementina, Universidad de Antioquia, 2004.

[15] E. Alarcón, L. Correa, C. Montes, A.L. Villa, Nopol production over Sn-MCM-41 synthesized by diffrent procedures – solvent effects, Microporous Mesoporous Mater. 136 (2010) 59–67.

[16] C.T. Kresge, M.E. Leonowicz, W.J. Roth, J.C. Vartuli, J.S. Beck, Ordered mesoporous molecular sieves synthesized by a liquid-crystal template mechanism, Nature 359 (1992) 710–712.

[17] F. Carniato, C. Bisio, G. Paul, G. Gatti, L. Bertinetti, L. Marchese, On the hydrothermal stability of MCM-41 mesoporous silica nanoparticles and the preparation of luminescent materials, J. Mater. Chem. 20 (2010) 5504–5509.

[18] A.T. Blomquist, R.J. Himics, Terpene-formaldehyde reactions. II. d-Limonene, J. Org. Chem. 33 (1968) 1156–1159.

[19] E. Grajales, E.A. Alarcón, A.L. Villa, Kinetics of depolymerization of paraformaldehyde obtained by thermogravimetric analysis, Thermochim. Acta 609 (2015) 49–60.

[20] M. Grün, K.K. Unger, A. Matsumoto, K. Tsutsumi, Novel pathways for the preparation of mesoporous MCM-41 materials: control of porosity and morphology, Microporous Mesoporous Mater. 27 (1999) 207.

[21] A.L. Villa, L.F. Correa, E.A. Alarcón, Kinetics of the nopol synthesis by the Prins reaction over tin impregnated MCM-41 catalyst, Chem. Eng. J. 215–216 (2013) 500–507.

[22] A.J.C.K. Chaudhari, T.K. Das, P.R. Rajmohanan, K. Lazar, S. Sivasanker, Synthesis, characterization, and catalytic properties of mesoporous tin-containing analogs of MCM-41, J. Catal. 183 (1999) 281–291.

[23] H.M. Mody, S. Kannan, H.C. Bajaj, V. Manu, R.V. Jasra, A simple room temperature synthesis of MCM- 41 with enhanced thermal and hydrothermal stability, J. Porous Mater. 15 (2008).

[24] E.A. Alarcón, A.L. Villa, C. Montes de Correa, Characterization of Sn- and Zn-loaded MCM-41 catalysts for nopol synthesis, Microporous Mesoporous Mater. 122 (2009) 208–215.

[25] D. Ford, E. Simanek, D. Shantz, Engineering nanospaces: ordered mesoporous silicas as model substrates for building complex hybrid materials, Nanotechnology 16 (2005) 458–475.

[26] S. Chaliha, K.G. Bhattacharyya, Wet oxidative method for removal of 2,4,6-tri-chlorophenol in water using Fe(III), Co(II), Ni(II) supported MCM41 catalysts, J. Hazard Mater. 150 (2008) 728–736.

[27] R.Y. Abrokwah, V.G. Deshmane, D. Kuila, Comparative performance of M-MCM-41 (M: Cu, Co, Ni, Pd, Zn and Sn) catalysts for steam reforming of methanol, J. Mol. Catal. A Chem. 425 (2016) 10–20.

[28] F. Adam, T.S. Chew, A facile template-free room temperature synthesis of mesoporous wormlike nickel phyllosilicate, Open Colloid Sci. J. 5 (2012) 1–4.

[29] M.P. Pachamuthu, K. Shanthi, R. Luque, A. Ramanathan, SnTUD-1: a solid acid catalyst for three component coupling reactions at room temperature, Green Chem. 15 (2013) 2158–2166.

[30] R. Rajalakshmi, R. Maheswari, A. Ramanathan, Characterization and activity of novel tin incorporated ordered cubic mesoporous silicate , Sn-KIT-6, Mater. Res. Bull. 75 (2016) 224–229.

[31] Classification of solvents, in: C. Reichardt, T. Welton (Eds.), Solvents Solvent Efects Org. Chem., fourth ed., Wiley-VCH, Weinheim, 2011, pp. 65–99.

[32] A. Viloria, M.J. Hidalgo, I. Aguas, E. Alarcón, A.L. Villa, Síntesis de Homolimonenol mediante la Reacción de Prins usando Sn-MCM-41 Como Catalizador. XXVI Congr. Iberoam. Catálisis, Coimbra, Portugal, 2018, p. 2434.